Electron-lattice interactions in the perovskite $LaFe_{0.5}Cr_{0.5}O_3$ characterized by optical spectroscopy and LDA+U calculations

Jakob Andreasson,[1,*] Joakim Holmlund,[1] Stefan G. Singer,[2] Christopher S. Knee,[3] Ralf Rauer,[1] Benjamin Schulz,[2] Mikael Käll,[1] Michael Rübhausen,[2] Sten-G. Eriksson,[4] Lars Börjesson,[1] and Alexander Lichtenstein[2]

[1]*Department of Applied Physics, Chalmers University of Technology, Göteborg, Sweden SE-41296*

[2]*Institut für Angewandte Physik, Universität Hamburg, Hamburg, Germany D-20355*

[3]*Department of Chemistry, University of Gothenburg, Göteborg, Sweden SE-41296*

[4]*Department of Environmental Inorganic Chemistry, Chalmers University of Technology, Göteborg, Sweden SE-41296*

(Received 31 March 2009; revised manuscript received 5 June 2009; published 4 August 2009)

We use resonance Raman scattering (incident photon energies between 1.8 and 4.13 eV), LDA+U calculations, spectroscopic ellipsometry, and oblique IR reflectivity to characterize the strong electron-phonon interactions in the disordered perovskite $LaFe_{0.5}Cr_{0.5}O_3$. When the photon energy coincides with a Cr to Fe Mott-Hubbard transfer gap around 2.4 eV the electron-phonon interaction is manifested by a Franck-Condon effect with exceptional first- and higher order scattering of a local oxygen breathing mode. At higher incident energies we observe a superposition of Franck-Condon scattering and Fröhlich interaction induced infrared active longitudinal optical two-phonon scattering activated mainly by O to Fe charge transfer. Our results establish $LaFe_{0.5}Cr_{0.5}O_3$ as a model compound for research on electron-phonon interactions in strongly correlated complex systems and show that Franck-Condon scattering in complex solids is not limited to Jahn-Teller active compounds.

DOI: 10.1103/PhysRevB.80.075103 PACS number(s): 71.35.Aa, 71.35.Gg, 71.38.Ht

I. INTRODUCTION

The nature of the interactions among electronic, structural, magnetic, and orbital properties in transition-metal (TM) oxides remains an active field of research.[1–3] Driven by their role in the colossal magnetoresistance (CMR) effect in the mixed-valence manganites, the orbitally mediated electron-phonon (el-ph) interactions are of particular importance.[4,5] Additional interest was generated with the prediction of an orbiton excitation in orbitally ordered $LaMnO_3$ made by Allen and Perebeinos[6,7] and the reported observation of an orbital wave excitation with an energy of about 150 meV in $LaMnO_3$.[8] This initial interpretation was soon challenged by a model based on el-ph interactions where the modes of interest were assigned to second-order features of Franck-Condon (FC) multiphonon scattering.[9,10] Recently, strong experimental evidence for the phonon origin of the 150 meV excitation in $LaMnO_3$ and similar compounds has been presented.[11,12] However, the complexity of the first- and higher order Raman spectra in the manganites complicates the mode assignment[11–13] and makes them unfavorable for detailed studies of el-ph interaction in complex oxide materials. Nevertheless, identification of a suitable model system for el-ph interaction in TM oxides would be of great value since it would serve as a sensitive probe of the interactions among local charge, spin, orbital, and lattice excitations and global properties in correlated systems.

We have previously reported the presence of a FC multiphonon effect in $LaFe_{0.5}Cr_{0.5}O_3$ (Ref. 14) and characterized in detail the higher order Raman-active scattering in $LaFe_{1-x}Cr_xO_3$ ($0.02 \leq x \leq 0.98$), $LaFeO_3$, and $LaCrO_3$ using a photon energy of $\hbar\omega = 2.41$ eV ($\lambda = 514$ nm).[15] In particular we have shown that the presence of FC scattering is critically sensitive to the observation of both Fe and Cr on the perovskite lattice *B* sites.[15] We have also reported that optical photons cause a simultaneous Fröhlich interaction (FI) induced longitudinal optical (IR LO) two-phonon activation and FC scattering in compounds with high Fe contents.[15]

Here we use a combination of experimental techniques and calculations to establish that the FC effect present for visible (VIS) wavelengths in the mixed *B* site compounds originates from a Cr to Fe Mott-Hubbard transition in locally ordered regions of $LaFe_{0.5}Cr_{0.5}O_3$. Further, for UV wavelengths the resonance profile of the scattering response indicates a superposition of FC and FI activated IR LO two-phonon scattering similar to that seen for optical photons in Fe-rich compounds. The present observations verify the close relation among chemical composition, electronic structure, and optical resonances and show that the FC effect in complex materials is not limited to compounds containing Jahn-Teller (JT) active *B*-site TM ions with partially filled e_g orbitals.

II. EXPERIMENTAL

The $LaFe_{0.5}Cr_{0.5}O_3$ sample is a polycrystalline pellet prepared by solid-state sintering. It adopts a pseudocubic structure of orthorhombic symmetry (space-group D_{2h}^{16}, *Pnma*). Indications of local *B*-site (Fe and Cr) rocksalt ordering has been observed in this sample, and antiferromagnetic (AFM) spin ordering occurs below $T_N = 265$ K. Further structural and magnetic properties are discussed in detail elsewhere.[14–16]

The main part of the resonance study (from $\hbar\omega = 2.18$ to 4.13 eV) was carried out on a custom designed UT3 Raman spectrometer (McPherson). The spot size was less than 20 μm in diameter covering an array of randomly oriented single crystallites. For the resonance study the sample was mounted in air, while for the temperature study it was mounted in a He flow cryostat. The beam power at the

sample was held below 10 mW. Additional spectra ($\hbar\omega$ =2.41, 1.92, and 1.82 eV) were collected using a DILOR-XY800 spectrometer with a spot size of about 50 μm and laser power below 10 mW. In both cases parallel relative polarizations of the incoming and scattered light were used. The spectra obtained with the two spectrometers were normalized using the $\hbar\omega$=2.41 eV measurements. The scattered signals were recorded using liquid-nitrogen-cooled multichannel charge coupled device (CCD) cameras. The resonance measurements have been corrected for sample and spectrometer effects.[17] These corrections include a factor related to the wavelength dependence of the scattering volume and the response of the spectrometer. The resulting quantity is directly proportional to the Raman response function. We do not include any assumption on the energy dependence of the vertex such as the $1/\omega^4$ factor present in the expression for the Raman intensity according to the simplified dipole approximation. All Raman spectra have been compensated for the thermal Bose-Einstein factor and are shown with vertical offsets for clarity.

The spin-density functional theory (SDFT) calculations were done using the LMTART program.[18] We applied the full-potential linear muffin-tin orbital (FP-LMTO) approximation with additional correlation treatments (LDA+U, U=3 eV). The lattice parameters used for the calculations are (in *Pnma* setting with long *b* axis) *a*=5.52 Å, *b*=7.81 Å, and *c* =5.54 Å. Further structural data are given in Ref. 16. The calculations were performed for the high-spin (HS) phase of a *B*-site ordered system (rocksalt ordering of Fe and Cr ions) with AFM spin orientation. Since the magnetic ordering does not affect the multiphonon spectra,[14,15] the corresponding spin-up and -down channels of the electronic partial density of states (eDOS) were combined.

Parallel polarized room-temperature angle-dependent reflectivity measurements were done at 20 and 70° angles using a Spectra Tech Series 500 specular reflectance accessory inserted in the infrared beam path of a Bruker 66 interferometer. The radiation was polarized with a polarizer made of a gold wire grid on a KRS-5 substrate. The optical-absorption spectrum was obtained by spectroscopic ellipsometry performed on a polished sample at room temperature.[14]

III. RESULTS AND DISCUSSION

The resonance Raman scattering (RRS) performed on $LaFe_{0.5}Cr_{0.5}O_3$ reveals resonant enhancements of the first- and higher order scattering in the VIS and UV energy regions (Fig. 1). For photon energies between 2.18 and 2.54 eV (wavelengths between 568 and 488 nm) a characteristic series of FC modes is observed. For this FC scattering the integrated intensity of the second-order excitation is about 50% of that of the first-order mode (Fig. 1, inset), and a relatively strong third-order scattering at about 2100 cm^{-1} is seen. As the photon energy is increased the FC resonance fades, and at $\hbar\omega$=3.00 eV a weakened first-order excitation is followed by a weak second-order mode and no third-order scattering (Fig. 1). The nature of the low energy phonon modes has been discussed elsewhere.[15]

Increasing the photon energy to between 3.27 and 3.71 eV activates a scattering response characterized by dominant

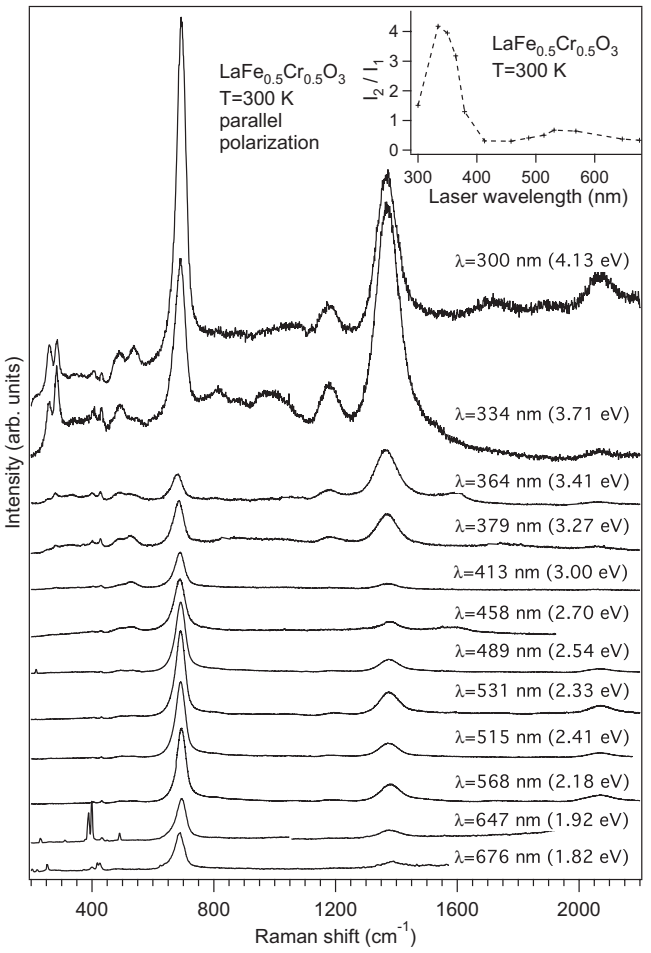

FIG. 1. Spectra showing the first- to second- or third-order Raman scattering in $LaFe_{0.5}Cr_{0.5}O_3$ obtained at room temperature using excitation energies in the visible and UV regions. Inset shows the relative integrated intensity between the dominant first- and second-order excitations (I_1 at about 700 cm^{-1} and I_2 at about 1400 cm^{-1}) as a function of laser wavelength.

second-order excitation (Fig. 1 and inset). The nature of this resonance is discussed further below, where it is identified as a FI induced IR LO two-phonon scattering. This IR LO two-phonon resonance still influences the spectrum obtained with $\hbar\omega$=4.13 eV, the highest photon energy used in this study. However, for this photon energy it is clear that the characteristic FC scattering profile reappears, including a prominent third-order mode (Fig. 1, top spectrum).

The resonance profiles of the integrated intensities of the first-, second-, and third-order scatterings are summarized in Fig. 2. Here we also show the real part of the optical conductivity tensor σ_1, which is proportional to the effective number of electrons excited by photons of respective energy. Thus, the similarity between the resonance profiles and σ_1 seen in Fig. 2 effectively links the appearance of RRS to electronic processes in the compound.

To identify the electronic processes associated with the experimentally observed optical absorption and Raman resonances, we compare the detected σ_1 and RRS profiles (Fig. 2) with the calculated electronic transition probabilities. The transition probabilities [Fig. 3(b)] are proportional to the

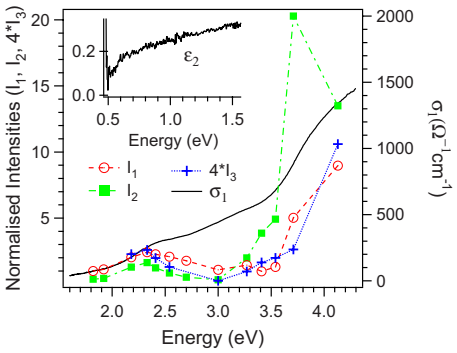

FIG. 2. (Color online) Resonance Raman-scattering profiles for the first-, second-, and third-order scattering of the oxygen breathing mode compared with the optical-absorption spectrum (σ_1). Normalized integrated intensities of the first, second, and fourth times the third-order modes (I_1, I_2, and 4^*I_3) are represented by open rings, filled squares, and plus signs, respectively. Activation of resonant scattering around $\hbar\omega$=2.4 eV and above 3.3 eV coincides with broad absorption bands at these energies. Integrated intensities are normalized in such a way that the weakest first-order scattering ($\hbar\omega$=1.82 eV) has value of 1. Inset shows the low-energy section of ε_2 (the imaginary part of the dielectric function) where an experimental indication of the band gap is seen at about 0.5 eV.

joint density of states (JDS) normalized by the energy (JDS/$\hbar\omega$). The JDS results from a simple convolution of the corresponding occupied and unoccupied eDOS seen in Fig. 3(a) and is directly proportional to σ_1.[19] The eDOSs were calculated using the FP-LMTO with additional correlation treatment (LDA+U, U=3 eV).

In the calculations of the eDOS the band gap of about 0.6 eV separates the occupied states of the Cr band close to E_F and the unoccupied Fe states centered in the band at about 1.0 eV [Fig. 3(a)]. An indication of this band gap is observed

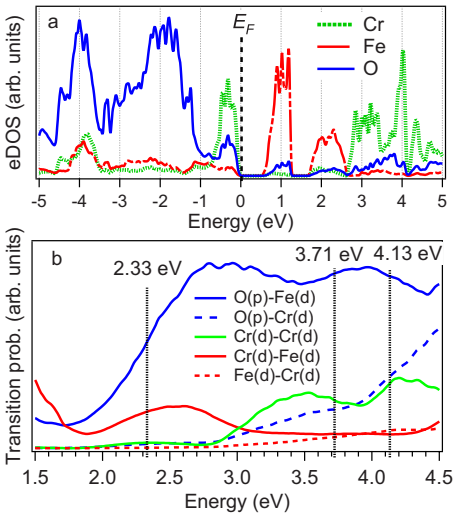

FIG. 3. (Color online) (a) Calculated partial electronic density of states. (b) The electronic transition probabilities proportional to the normalized joint density of states obtained from a convolution of the occupied and unoccupied states seen in Fig. 3(a). Vertical lines indicate resonant Raman scattering according to experiments (FC at 2.33 eV, IR LO two-phonon at 3.71 eV, and FC at 4.13 eV)

experimentally in the low-energy region of the imaginary part of the dielectric function (Fig. 2 inset). In addition to the first Fe band at 1 eV, a second well-defined Fe band is centered around 2.1 eV [Fig. 3(a)]. The distance between the center of the Cr band below the E_F and the center of this second Fe band is about 2.4 eV, and we propose that a Mott-Hubbard transition between these two bands is responsible for the optical absorption seen around 2.4 eV in the optical data (Fig. 2) and the resonant activation of the FC scattering that appears for excitation energies around 2.3 eV (Figs. 1 and 2).

Due to the difference in characteristic time scales of electronic and lattice dynamics (about 10^{-15} and 10^{-12} s, respectively) a coupling mechanism is required for the electronic excitation to couple to the lattice. Within the Kramers-Heisenberg-Dirac (KDH) formalism[20] the transition probabilities to the higher order excitations of the involved vibrational excitations depend on the overlap between the vibrational wave functions in the ground, intermediate, and final states of the Raman process. As a result, FC scattering may occur in any sample if a self-trapping mechanism causes a displacement of the excited-state potential parabola that increases this overlap and as a consequence increases the probability of the system ending up in highly excited vibrational states.[20]

For TM oxides it has been predicted that self-trapping of a local electronic excitation by an oxygen rearrangement may result in the activation of strong FC multiphonon scattering.[7] This self-trapping is traditionally mediated by the orbital overlap between the TM d and the O p electron orbitals. In the much studied manganites the FC scattering is activated by an intrasite e_g to e_g excitation across the JT gap and affects the modes with JT-like normal coordinates. Thus, it has been assumed that the d^4 electronic configuration is instrumental for the appearance of FC scattering in transition-metal oxides.[14,15]

Given that the presence of FC scattering in $LaFe_{1-x}Cr_xO_3$ is critically sensitive to a presence of both Fe and Cr on the B site[15] and that the electronic ground state in HS $LaFe_{0.5}Cr_{0.5}O_3$ has Fe(3+)d^5 and Cr(3+)d^3 configuration, we have previously proposed that the initial step in the self-trapping process that eventually activates the FC scattering around 2.4 eV is a Fe to Cr Mott-Hubbard transition.[14,15]

However, while our present calculations (Fig. 3) show a strong presence of a Cr to Fe transition channel that well matches the profile of the observed Raman resonance around 2.3 eV [from states in the Cr band centered around −0.3 eV to the Fe band centered around 2.1 eV (Figs. 2 and 3)], there is no evidence in the present calculations for extensive Fe to Cr transition. This leads us to now propose that the initial step in the activation of the FC scattering is a Cr to Fe Mott-Hubbard transition that occurs in the locally ordered regions of the sample. Thus, the present results indicate that the FC scattering occurs in a local Fe(2+)d^6 Cr(4+)d^2 environment. Once this excitation is trapped by an orbitally mediated lattice rearrangement the Coulomb interaction of the new local charge state (with 2+ and 4+ nearest neighbors instead of 3 + and 3+) couples to the intrinsic oxygen breathing mode and activates the FC scattering.[14]

With higher excitation energies, between 3.3 and 3.7 eV, a remarkable increase in the second-order scattering region oc-

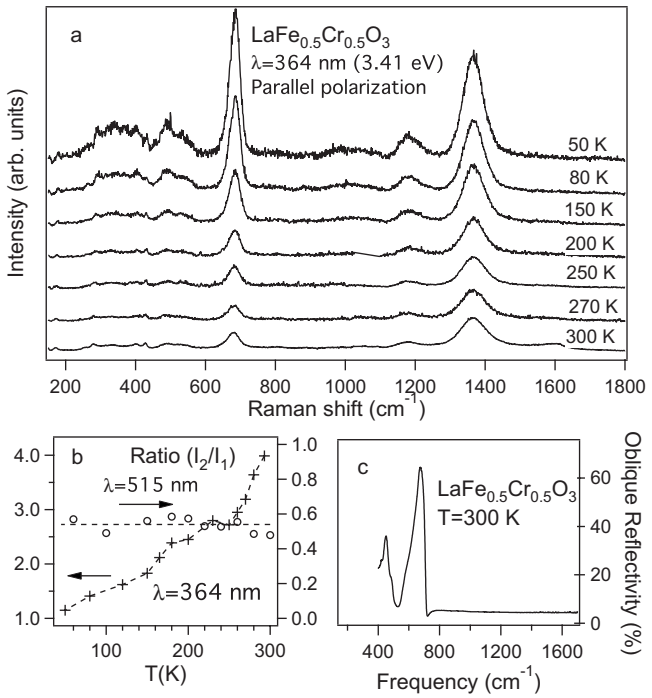

FIG. 4. (a) Temperature dependence of the first- and second-order Raman spectra of $LaFe_{0.5}Cr_{0.5}O_3$ at the mid-UV resonance using $\hbar\omega$=3.41 eV and parallel polarization. (b) Temperature dependence of the ratio between the dominant first- and second-order excitations (I_2/I_1) for the visible wavelength λ=515 nm (open rings) and UV wavelength λ=364 nm (plus signs). These wavelengths correspond to photon energies of $\hbar\omega$=2.41 eV and $\hbar\omega$=3.41 eV, respectively. (c) Oblique reflectivity for incident angle at 70° and parallel configuration. IR LO modes at about 450 and 675 cm^{-1}.

curs (Figs. 1 and 2). The temperature dependence of the first- and second-order scatterings measured at 3.41 eV differs substantially for the FC resonance activated using VIS photon energies [Fig. 4(b)]. For the FC resonance at $\hbar\omega$=2.41 eV, I_2/I_1 is independent of temperature with an average value about 0.5. In contrast, using UV $\hbar\omega$=3.41 eV photons, the integrated intensity of the first-order peak increases more rapidly with decreasing temperature than does that of the second-order peak [Fig. 4(a)]. This causes a significant decrease in the ratio I_2/I_1 for λ=364 nm ($\hbar\omega$=3.41 eV) as temperature is lowered [Fig. 4(b)].

Observations of strong second-order scattering with little or no first-order scattering have previously been made in several TM oxides.[15,21,22] In particular we have reported that the first- and higher order scattering present using 2.41 eV photons on Fe-rich $LaFe_{1-x}Cr_xO_3$ is remarkably similar to that activated by 3.71 eV photons in $LaFe_{0.5}Cr_{0.5}O_3$.[15] In many cases such scattering is associated with two-phonon activation of either FI induced IR LO modes activated by O to TM charge transfer[15,21,22] or phDOS scattering activated by impurity-related local symmetry breaking.[11] In $LaFe_{0.5}Cr_{0.5}O_3$ an IR LO mode at about 675 cm^{-1} is also seen in IR oblique reflectivity measurements performed at room temperature [Fig. 4(c)]. Thus, combining our present and previous findings[15] we conclude that the strong second-order scattering that appears for UV frequencies in $LaFe_{0.5}Cr_{0.5}O_3$ is generated by a FI induced two-phonon activation of an IR LO phonon activated by O to Fe charge transfer.

At even higher energies the characteristic FC scattering reappears and dominates for $\hbar\omega$=4.13 eV (Fig. 1 top spectrum). From the present calculations it is clear that the FC scattering present for 4.13 eV is not generated by the same simple Cr to Fe transition responsible for the VIS FC resonance (Fig. 3). Several electronic processes increase in strength at UV energies (most notably O to Fe, O to Cr, and Cr to Cr) but the Cr to Fe transition is very weak (Fig. 3). However a combination of Cr-Cr and O-Fe transitions in a local region could generate the same local Fe(2+)d^6 Cr(4+)d^2 environment that is responsible for the VIS FC resonance.

IV. CONCLUSIONS

We analyze the resonant el-ph interactions in the perovskite $LaFe_{0.5}Cr_{0.5}O_3$ using a combination of experiments and LDA+U calculations. The simplicity of the first- and higher order Raman spectra and the exceptional magnitude of the Franck-Condon scattering in the easily attainable visible region make $LaFe_{0.5}Cr_{0.5}O_3$ an ideal model system for studies of electron-phonon interactions in complex materials. For UV Raman excitation frequencies we observe a superposition of Fröhlich interaction induced activation of IR LO two-phonon and Franck-Condon scattering. A similar resonance mixing has been observed in Fe-rich $LaFe_{1-x}Cr_xO_3$, and the present observations verify the close relations among chemical composition, electronic structure, and optical properties. The present observations show that strong electron-phonon interactions in complex materials are not limited to Jahn-Teller active compounds and that the Fe-Cr system is appealing for studies on the competition/coexistence of different electron-phonon interactions.

ACKNOWLEDGMENTS

The support of the Swedish Research Council and the Foundation for Strategic Research (Complex Oxide program) is gratefully acknowledged. We acknowledge support from the DFG via the Graduiertenkolleg 1286. We are thankful to N. E. Massa at Universidad Nacional de La Plata, La Plata, Argentina for performing the IR reflectivity measurements, M. Bastjan at Universität Hamburg, Hamburg, Germany for performing the ellipsometry, and P. Johansson at Örebro University, Örebro, Sweden for helpful discussions.

*Present address: Department of Cell and Molecular Biology, Uppsala University, Uppsala, Sweden.

[1] E. Dagotto and Y. Tokura, MRS Bull. **33**, 1037 (2008).
[2] Y. Tokura, Phys. Today **56** (7), 50 (2003).
[3] C. Sen, G. Alvarez, and E. Dagotto, Phys. Rev. Lett. **98**, 127202 (2007).
[4] A. J. Millis, B. I. Shraiman, and R. Mueller, Phys. Rev. Lett. **77**, 175 (1996).
[5] N. A. Babushkina, L. M. Belova, O. Yu. Gorbenko, A. R. Kaul, A. A. Bosak, V. I. Ozhogin, and K. I. Kugel, Nature (London) **391**, 159 (1998).
[6] P. B. Allen and V. Perebeinos, Phys. Rev. Lett. **83**, 4828 (1999).
[7] V. Perebeinos and P. B. Allen, Phys. Rev. B **64**, 085118 (2001).
[8] E. Saitoh, S. Okamoto, K. T. Takahashi, K. Tobe, K. Yamamoto, T. Kimura, S. Ishihara, S. Maekawa, and Y. Tokura, Nature (London) **410**, 180 (2001).
[9] R. Krüger, B. Schulz, S. Naler, R. Rauer, D. Budelmann, J. Bäckström, K. H. Kim, S.-W. Cheong, V. Perebeinos, and M. Rübhausen, Phys. Rev. Lett. **92**, 097203 (2004).
[10] L. Martín-Carrón and A. de Andrés, Phys. Rev. Lett. **92**, 175501 (2004).
[11] M. N. Iliev, V. G. Hadjiev, A. P. Litvinchuk, F. Yen, Y.-Q. Wang, Y. Y. Sun, S. Jandl, J. Laverdiére, V. N. Popov, and M. M. Gospodinov, Phys. Rev. B **75**, 064303 (2007).
[12] J. Laverdière, S. Jandl, A. A. Mukhin, and V. Yu. Ivanov, Eur. Phys. J. B **54**, 67 (2006).
[13] K.-Y. Choi, P. Lemmens, G. Güntherodt, Yu. G. Pashkevich, V. P. Gnezdilov, P. Reutler, L. Pinsard-Gaudart, B. Büchner, and A. Revcolevschi, Phys. Rev. B **72**, 024301 (2005).
[14] J. Andreasson, J. Holmlund, C. S. Knee, M. Käll, L. Börjesson, S. Naler, J. Bäckström, M. Rübhausen, A. K. Azad, and Sten-G. Eriksson, Phys. Rev. B **75**, 104302 (2007).
[15] J. Andreasson, J. Holmlund, R. Rauer, M. Käll, L. Börjesson, C. S. Knee, A. K. Eriksson, Sten-G. Eriksson, M. Rübhausen, and R. P. Chaudhury, Phys. Rev. B **78**, 235103 (2008).
[16] A. K. Azad, A. Mellergård, S.-G. Eriksson, S. A. Ivanov, S. M. Yunus, F. Lindberg, G. Svensson, and R. Mathieu, Mater. Res. Bull. **40**, 1633 (2005).
[17] B. Schulz, J. Bäckström, D. Budelmann, R. Maeser, M. Rübhausen, M. V. Klein, E. Schoeffel, A. Mihill, and S. Yoon, Rev. Sci. Instrum. **76**, 073107-1 (2005).
[18] S. Y. Savrasov and D. Y. Savrasov, Phys. Rev. B **46**, 12181 (1992).
[19] W. Y. Liang and A. R. Beal, J. Phys. C. **9**, 2823 (1976).
[20] *Handbook of Vibrational Spectroscopy*, edited by J. M. Chalmers and P. R. Griffiths (Wiley, New York, 2002), Vol. 1.
[21] M. V. Abrashev, A. P. Litvinchuk, C. Thomsen, and V. N. Popov, Phys. Rev. B **55**, R8638 (1997).
[22] J. Holmlund, J. Andreasson, C. S. Knee, J. Bäckström, M. Käll, M. Osada, T. Noji, Y. Koike, M. Kakihana, and L. Börjesson, Phys. Rev. B **74**, 134502 (2006).